Journal of Materials Science Research; Vol. 6, No. 2; 2017
ISSN 1927-0585 E-ISSN 1927-0593
Published by Canadian Center of Science and Education

Deposition of Transition Temperature Controlled Thermochromic $Nd_xSm_{1-x}NiO_3$ Films by Spin Coating

Hidetoshi Miyazaki[1], Yusuke Maejima[1] & Yuki Makinose[1]

[1] Interdisciplinary Graduate School of Science and Engineering, Shimane University, Nishikawatsu, Japan

Correspondence: Hidetoshi Miyazaki, Interdisciplinary Graduate School of Science and Engineering, Shimane University, 1060, Nishikawatsu, Matsue, Shimane, 690-8504, Japan. E-mail: miya@riko.shimane-u.ac.jp

Received: March 9, 2017 Accepted: March 20, 2017 Online Published: March 27, 2017

doi:10.5539/jmsr.v6n2p79 URL: https://doi.org/10.5539/jmsr.v6n2p79

Abstract

The precursor samarium nickelate or samarium-neodimium nickelate films were fabricated by a spin coating method using Sm-Ni or Nd-Sm-Ni aqueous solutions, and $SmNiO_3$ and $Nd_{0.5}Sm_{0.5}NiO_3$ films were obtained by heat-treatment of the precursor films at 750 °C in oxygen atmosphere. The resulting $SmNiO_3$ and $Nd_{0.5}Sm_{0.5}NiO_3$ films showed an electrical transition with the transition temperatures of 124.0 and 32.5 °C, respectively. Both of the films showed optical thermochromic properties at the above mentioned transition temperatures.

Keywords: thermochromic, $SmNiO_3$, film, metal-insulator transition

1. Introduction

Lots of energy-efficient window materials have been investigated, including electrochromic materials (Granqvist, 2007; Yang et al., 2012), thermochromic materials (Takahashi, Hibino, & Kudo, 1996; Miyazaki & Yasui, 2006; Granqvist, 2007) and photochromic materials (Armistead & Stookey, 1964; Scarminio, Lourenco, & Gorenstein, 1997; Granqvist, 2007). These window materials realize to decrease environmental loads concerning with the energy for air conditioning. VO_2 has been widely investigated for application of thermochromic materials because of its metal-insulator transition property, and the transition temperature can be controlled close to room temperature by the other element addition. The other materials such as $SmNiO_3$ assume to be applied for a thermochromic window since $SmNiO_3$ also undergoes a metal-insulator transition (Lacorre et al., 1991; Pérez-Cacho et al., 1999; Nikulin et al., 2004; Girardot et al., 2008).

$SmNiO_3$ (SN) undergoes a reversible metal-semiconductor transition at around 127 °C, resulting in great changes in its electrical properties (Lacorre et al., 1991; Pérez-Cacho et al., 1999; Nikulin et al., 2004; Girardot et al., 2008). The transition temperature of $NdNiO_3$ is around –73 °C, and the transition temperature of a mixture phase $Sm_{1-x}Nd_xNiO_3$ varies continuously with changing Nd contents (Nikulin et al., 2004). If x=0.5 in $Sm_{1-x}Nd_xNiO_3$, the transition temperature on the electrical resistivity was 24 °C (Nikulin et al., 2004) which value is close to room temperature. Thus, the $Sm_{0.5}Nd_{0.5}NiO_3$ film can be applied to a thermochromic window. Previously, there have not been reported on Nd doped $SmNiO_3$ films for thermochromic window applications, and we have carried out it in the present study.

In previous our reports, we fabricated $SmNiO_3$ films by a spin coating method using a samarium nickelate solution, and evaluated an optical thermochromic property for the films (Miyazaki et al., 2013). On the spin coating method, an elementary composition of the resulting films can be controlled by changing the source sample ratios in the solution, furthermore the film thickness can be controlled by a concentration of the source solution and coating numbers. Thereby, we employed a spin coating method to prepare Nd doped $SmNiO_3$ films. In the previous investigation, we have not measured a transition temperature of the film, and have not controlled the transition temperature. In the present study, we fabricated transition temperature controlled $SmNiO_3$ films by Nd addition, and the target composition is $Sm_{0.5}Nd_{0.5}NiO_3$. We evaluated the transition temperature by measuring a temperature dependence of electrical resistivity, and observed the thermochromic property of the transition temperature controlled films.

2. Experimental

2.1 Preparation

Nickel nitrate ($Ni(NO_3)_2{\cdot}H_2O$), samarium acetate ($Sm(CH_3COO)_3$) and neodymium acetate ($Nd(CH_3COO)_3$) starting materials were dissolved in distilled water to produce a $0.25M{\cdot}L^{-1}$ solution with an (Sm and Nd):Ni elemental ratio of 1:1. Poly vinyl alcohol (PVA) was mixed into the precursor solution with 0.1 wt% contents to increase its viscosity. Precursor thin films were then fabricated on quartz substrate by a spin-coating method using the above mentioned precursor solution. The films were dried at 150 °C for 10 min and then pre-annealed at 400 °C for 10 min to remove residual organics. These processes were repeated 10 times, after which the films were annealed at 750 °C for 2 h in oxygen stream using an electric furnace.

2.2 Characterization

The crystal structure of the films was determined using X-ray diffraction (XRD, Miniflex; Rigaku Corp., Japan) at room temperature using CuKα radiation. The microstructure and the film thickness of the resulting films were observed using scanning electron microscopy (SEM, JSM–6510; JEOL, Japan). The resistivity of the resulting films was measured by 2-porobe method because of its high resistance. The radiative temperature was evaluated using a radiation thermometer (TMHX–CN; Japan sensor, Japan). The transmittance of the films was measured using a JASCO V–670 spectrophotometer at a wave length range in 200–2500 nm.

3. Results and Discussion

$SmNiO_3$ (SN) and $Nd_{0.5}Sm_{0.5}NiO_3$ (NSN) films were fabricated on silica glass substrates at 750 °C for 2h, and the XRD patterns for these films were shown in Figure 1. Both of the film consisted of a SNO main phase, and Sm_2O_3, Nd_2O_3 and unknown phase were observed secondary phases. Both of the films showed $SmNiO_3$ as a main phase, and these films were employed for measurement of the electrical and optical properties.

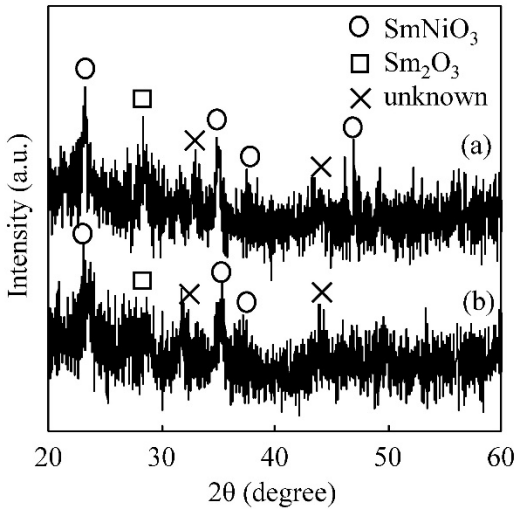

Figure 1. XRD patterns for the (a) $SmNiO_3$ and the (b) $Nd_{0.5}Sm_{0.5}NiO_3$ films, heat-treated at 750 °C in oxygen atmosphere.

Figure 2 depicts the cross sectional SEM images for the resulting SN and NSN films. Both of the films showed a flat surface with high dense. The film thickness of the SN and NSN films was 0.58 and 0.48 μm, respectively. Utilizing the film thickness value, the electrical resistivity of the films was measured. Figure 3 illustrates the resistivity of the resulting films. Though a gradient of the resistivity of the films changed beyond the transition temperature, the resistivity of both of the films increased with increase of temperature. Thus, both of the films showed a semiconducting phase at high temperature. Typically, $SmNiO_3$ powder has few oxygen defects when synthesized under a high oxygen pressure (5.0 MPa) (Miyazaki et al., 2013). This pressure is much higher than the 101.3 kPa (atmospheric pressure) used to fabricate the present SN films, which had a large amount of oxygen defects. Oxygen defects in SN causes low electron conductivity at the high temperature phase of the SN (Nikulin et al., 2004), and thus both of the films did not exhibit a metallic property at high temperature phase. The electrical resistivity of the films between the low temperature phase and high temperature phase varied, and, the transition

temperature of the films could be evaluated utilizing this phenomenon. The calculated transition temperature of the SN and NSN films were 124.0 and 32.5 °C, and the value of SN was close to the reported value, and the value of NSN was slightly higher than the reported value (Nikulin et al., 2004).

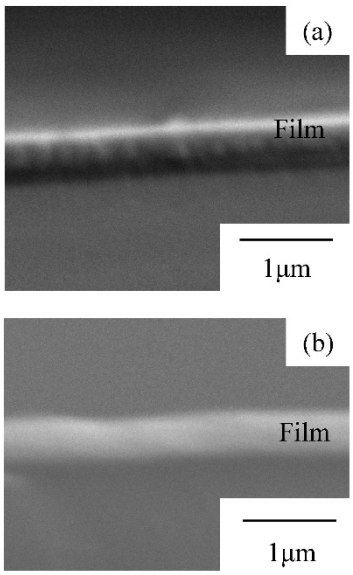

Figure 2. Cross sectional SEM images of the (a) $SmNiO_3$ and the (b) $Nd_{0.5}Sm_{0.5}NiO_3$ films

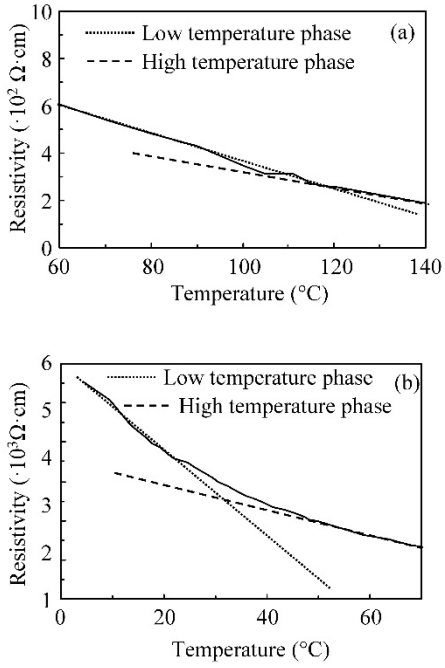

Figure 3. Temperature dependence of an electrical resistivity of the (a) $SmNiO_3$ and the (b) $Nd_{0.5}Sm_{0.5}NiO_3$ films

The radiative emissivity value of $SmNiO_3$ varies from the low temperature phase of 0.75 to the high temperature phase of 0.57, and the transition temperature can be also evaluated utilizing this property (Ha et al., 2012). Figure 4 presents the temperatures measured by a thermocouple (recorded on the abscissa axis) and a radiation thermometer (recorded on the vertical axis), and the radiative emissivity value of the detector was fixed "1" at all the temperature range. The radiation temperature of the SN and NSN films lowered around 123 and 33 °C because these materials underwent the phase transition at the temperatures. These evaluated transition temperatures almost coincided the transition temperatures measured from the electrical resistivity.

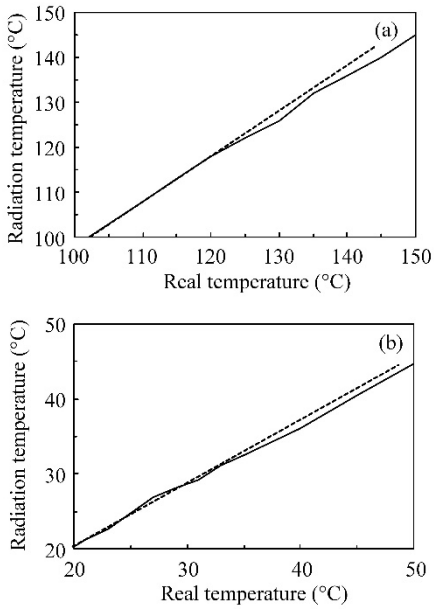

Figure 4. Correlation of a real and a radiative temperature of the (a) $SmNiO_3$ and the (b) $Nd_{0.5}Sm_{0.5}NiO_3$ films. The real and the radiative temperatures of films were measured by a thermocouple (the abscissa axis) and a radiation spectrometer (the vertical axis)

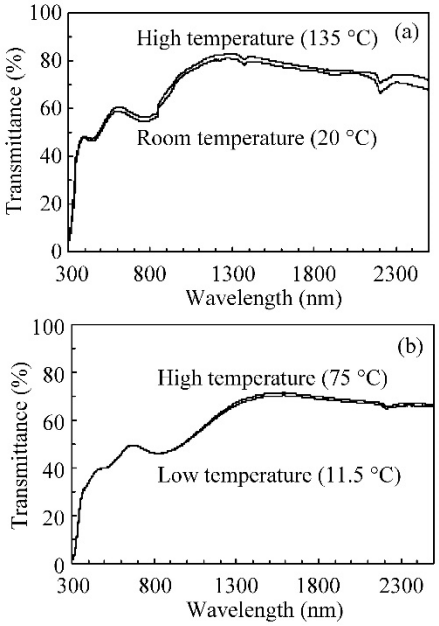

Figure 5. Transmittance of the (a) $SmNiO_3$ and the (b) $Nd_{0.5}Sm_{0.5}NiO_3$ films. The measurements were carried out at higher and lower than the transition temperatures

These results suggested that the obtained SN and NSN films showed a thermochromic property, thus we evaluated an optical thermochromic property for the films. Figure 5 shows transmittance spectra for the SN and NSN films at lower and higher temperatures of the transition temperature of the films. Transmittance of the films varied within the measured wavelength range of 1200–2500 nm between lower and higher temperatures of the transition temperatures, and exhibiting 5.74 and 0.91 % change in transmittance at 2400 nm. From the results of a temperature dependence of resistivity, it assumed that the electron carrier in both of the films increased with increase of temperature. Near IR light was scattered because of increasing carriers, and the optical thermochromism was observed for the resulting films.

4. Conclusion

$SmNiO_3$ (SN) and $Nd_{0.5}Sm_{0.5}NiO_3$ (NSN) films were successfully fabricated by a spin coating method using Sm-Ni or Sm-Nd-Ni aqueous solutions. Though the resulting films showed a transition, the high-temperature phase did not show a metallic property. This result caused oxygen defects in the films because of not heat-treated in a high oxygen pressure. The transition temperatures of the SN and NSN films were 124.0 and 32.5 °C from the electrical property, and these films showed an optical thermochromic property. These results suggest that NSN film can be applied for the optical thermochromic window materials with the switching temperature of room temperature.

References

Armistead, W. H., & Stookey, S. D. (1964). Photochromic silicate glasses sensitized by silver halides. *Science*, *144*(3615), 150-154.

Girardot, C., Kreisel, J., Pignard, S., Caillault, N., & Weiss, F. (2008). Raman scattering investigation across the magnetic and metal-insulator transition in rare earth nickelate R NiO 3 (R= Sm, Nd) thin films. *Physical Review B*, *78*(10), 104101.

Granqvist, C. G. (2007). Transparent conductors as solar energy materials: A panoramic review. *Solar energy materials and solar cells*, *91*(17), 1529-1598.

Ha, S. D., Otaki, M., Jaramillo, R., Podpirka, A., & Ramanathan, S. (2012). Stable metal–insulator transition in epitaxial SmNiO 3 thin films. *Journal of Solid State Chemistry*, *190*, 233-237.

Lacorre, P., Torrance, J. B., Pannetier, J. S. A. I., Nazzal, A. I., Wang, P. W., & Huang, T. C. (1991). Synthesis, crystal structure, and properties of metallic PrNiO3: Comparison with metallic NdNiO3 and semiconducting SmNiO3. *Journal of Solid State Chemistry*, *91*(2), 225-237.

Miyazaki, H., & Yasui, I. (2006). Effect of buffer layer on VO x film fabrication by reactive RF sputtering. *Applied surface science*, *252*(23), 8367-8370.

Miyazaki, H., Kikitsu, S. I., Suzuki, H., Adachi, N., & Toshitaka, O. T. A. (2013). Fabrication of thermochromic SmNiO3 film deposited by spin-coating method from aqueous solution. *Journal of the Ceramic Society of Japan*, *121*(1409), 10-12.

Napierala, C., Edely, M., Laffez, P., & Sauques, L. (2009). Thermo-optical effect of Nd 0.3 Sm 0.7 NiO 3 ceramic in the infrared range. *Optical Materials*, *31*(10), 1498-1501.

Nikulin, I. V., Novojilov, M. A., Kaul, A. R., Maiorova, A. F., & Mudretsova, S. N. (2004). Synthesis and transport properties study of Nd 1− x Sm x NiO 3− δ solid solutions. *Materials research bulletin*, *39*(6), 803-810.

Nikulin, I. V., Novojilov, M. A., Kaul, A. R., Mudretsova, S. N., & Kondrashov, S. V. (2004). Oxygen nonstoichiometry of NdNiO 3− δ and SmNiO 3− δ. *Materials research bulletin*, *39*(6), 775-791.

Pérez-Cacho, J., Blasco, J., García, J., Castro, M., & Stankiewicz, J. (1999). Study of the phase transitions in. *Journal of Physics: Condensed Matter*, *11*(2), 405-415.

Scarminio, J., Lourenco, A., & Gorenstein, A. (1997). Electrochromism and photochromism in amorphous molybdenum oxide films. *Thin Solid Films*, *302*(1-2), 66-70.

Takahashi, I., Hibino, M., & Kudo, T. (1996). Thermochromic V1-xWxO2 thin films prepared by wet coating using polyvanadate solutions. *Japanese journal of applied physics*, *35*(4A), L438-L440.

Yang, L., Ge, D., Zhao, J., Ding, Y., Kong, X., & Li, Y. (2012). Improved electrochromic performance of ordered macroporous tungsten oxide films for IR electrochromic device. *Solar Energy Materials and Solar Cells*, *100*, 251-257.

Copyrights